Statistical modeling of interferometric signals in underwater applications

Gerard Llort Pujol, Christophe Sintes

Statistical modeling of interferometric signals in underwater applications

Gerard Llort and Christophe Sintes
Institut Télécom - Télécom Bretagne, Dpt ITI
CNRS UMR 3192 Lab-STICC
Technopôle Brest-Iroise - CS 83818
29238 Brest, France.

ABSTRACT

Current sonar and radar applications use interferometry to estimate the arrival angles of backscattered signals at time-sampling rate. This direction-finding method is based on a phase-difference measurement between two close receivers. To quantify the associated bathymetric measurement quality, it is necessary to model the statistical properties of the interferometric-phase estimator. Thus, this paper investigates the received signal structure, decomposing it into three different terms: a part correlated on the two receivers, an uncorrelated part and an ambient noise term.

This paper shows that the uncorrelated part and the noise term can be merged into a unique, random term damaging the measurement performance. Concerning the correlated part, its modulus can be modeled either as a random or a constant variable according to the type of underwater acoustic application. The existence of these two statistical behaviors is verified on real data collected from different underwater scenarios such as a horizontal emitter-receiver communication and a bathymetric seafloor survey. The physical understood of the resulting phase distributions makes it possible to model and simulate the interferometric-signal variance (associated with the measurement accuracy) according to the underwater applications through simple hypotheses.

Keywords: multilook fusion, interferometry, phase statistics, signal decomposition, bathymetric measurement.

1. INTRODUCTION

Several acoustic applications such as hydrography, mine detection or pipeline tracking require bathymetric measurements to estimate the seafloor local depths from the sonar depth, and thus, to retrieve accurately the seabed topography. Interferometry is an angle estimation method widely used today in both sonar[1] and radar[2] applications, providing very accurate measurements[3] of seabed or earth-surface relief. The principle of interferometric bathymetry lies on the spacing between two close receivers causing a phase difference between received signals. The direct relationship between the phase difference and the direction of arrival[3] makes it possible to transform each phase sample into an angular sample, allowing a continuous description of a target.

Interferometry is unfortunately affected by two main phenomena complicating the phase-delay estimation. The first one concerns the 2π phase ambiguity:[4] the phase difference is measured 2π modulo as soon as the inter-sensor spacing is larger than $\lambda/2$. Consequently, an interferometric-phase ambiguity removal turns out to be crucial in order to estimate the target elevation angle; otherwise, the averaged phase may be biased.[5] Several techniques for removing the interferometric phase ambiguity can be found in the literature for both radar and sonar systems.[6–9]

The second issue of interferometry lies on the existing noise. The main causes for phase degradation can be categorized into intrinsic noise, corresponding to phenomena responsible for the signal decorrelation, and external noise, additive to the actual backscattered echoes and directly affecting the bathymetry estimation without being

Further author information: (Send correspondence to G.L.)
G.L.: E-mail: gerard.llort@telecom-bretagne.edu
C.S.: E-mail: christophe.sintes@telecom-bretagne.edu

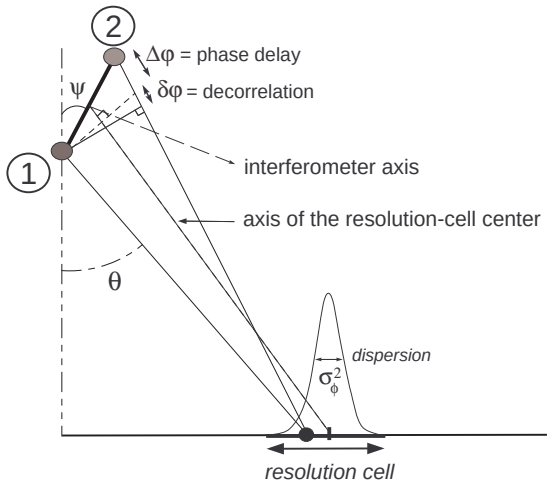

Figure 1. Geometry configuration of an interferometric measurement.

related to the phase-estimation processing in itself. These two types of noise may damage the interferometry processing and degrade the estimated bathymetry. In this paper, only the intrinsic phenomena[1,8,10] (such as the angular and spatial decorrelation, ambient noise or multipath interferences) are addressed, and the extrinsic phenomena (such as roll effects or water velocity fluctuations) are not considered.

The study of the decorrelation existing between two receivers is crucial for interferometric applications. Its importance is enhanced by the interferometric probability density function (PDF) and the resulting variance equation[11] since their shapes are completely characterized by the correlation coefficient as discussed later in Section 2.3. This coefficient relates the energy common to the two interferometric receivers to the whole energy, which can be split into a correlated part, an uncorrelated part and an ambient noise. We show in Section 2 that both the uncorrelated energy and the ambient noise are random processes; conversely, according to the underwater applications, the correlated part of the received energy can be considered either constant or random. This decomposition makes it possible to create two types of signals: random-modulus and constant-modulus partially-correlated signals. According to the assumption, the resulting phase-difference estimation will be more or less fluctuating, leading to a better or worse bathymetry. The analysis of the nature of interferometric signals is carried out in Section 2 where these two types of signals are confronted to real data collected in different underwater applications.

With the statement of these two types of signals, the following goal is to find a signal (or noise) model that simulates the reality. The classical additive model[12,13] consisting in a signal perturbed by an additive noise is a very useful mathematical approach, widely used in most seafloor mapping applications, but it may lack a physical meaning. Indeed, it can be quite difficult to draw conclusions about the backscattering process from this model. We present in Section 3, a more physical approach based upon a multiplicative-noise model that allows us to draw conclusions about the possible existence of a constant-modulus partially-correlated signal.

2. NATURE OF INTERFEROMETRIC SIGNALS

2.1 Signal recording

A bathymetric sonar signal ensonifies instantaneous resolution cells, geometrically defined by the beam width, steering angle and signal duration. The echo signal is sent back by elementary scatterers inside the resolution cell. The notion of *multilook* in radar applications arises when a given resolution cell is scanned several times at various observation dates. Thus, each time the resolution cell is illuminated, local scatterers with the same statistical properties randomly contribute to the wavefront backscattering process. Hence, N independent looks or snapshots are taken into account for measuring one elevation angle. The *single-look* case corresponds to a unique realization of a given observation.

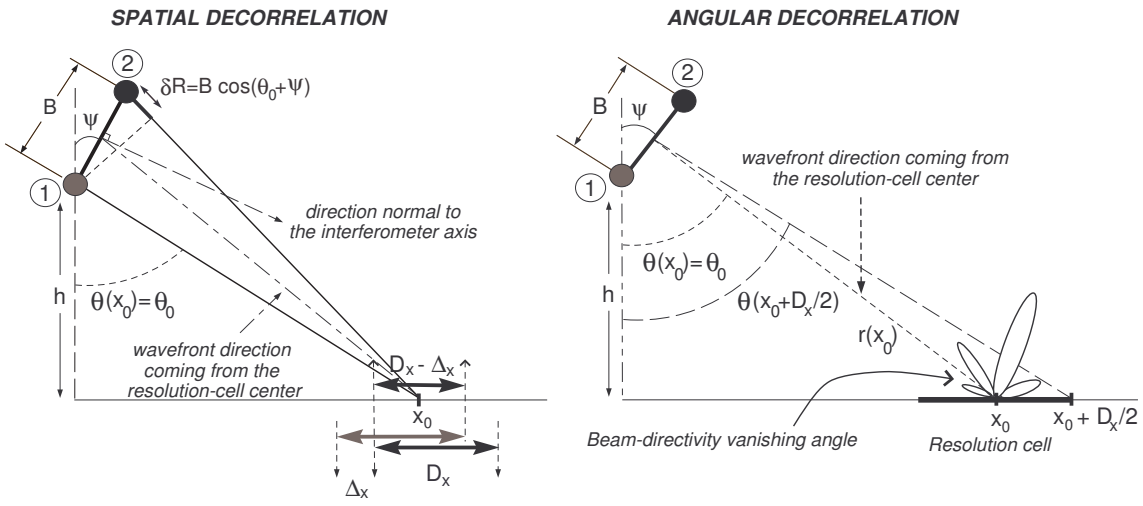

Figure 2. Definition of the parameters used to evaluate the spatial (left) and angular (right) decorrelation. It includes the two-way propagation distance $r(x_0)$, the arrival angle $\theta(x_0)$, the resolution cell of center x_0 and size D_x, and the sliding footprint Δ_x.

Practically, for bathymetric sonar systems, the usual strategy of coverage precludes to survey the same area several times for cost and efficiency reasons. Therefore, the multilook concept is slightly different: N interferometric samples are assumed to be close enough to a given sample under consideration for having the same properties in terms of statistics, radiation pattern, backscattering strength or topography; this amounts to saying, from a statistical point of view, that the same sample is seen several times.

In addition to the backscatter processes, other types of signals can be regarded. For instance, in underwater positioning applications[14] or in underwater acoustic communications,[15] the direct path between emitter and receiver (ideally without any reflection phenomenon) makes the received signal be more stable, or at least far less fluctuating, than backscattered signals. This is due to the fact that backscattered signals used in sonars arise from the contributions of an arbitrary number of scatterers, causing the fluctuating behavior. Conversely, signals in underwater positioning applications are received from one transmission path, yielding a more stable behavior. In practice, these two types of signals share some common degrading phenomena such as transmission loss, additive noise or multipath interferences that affect the phase-estimation variance.

2.2 Signal degradation

Several phenomena[1,10,16] such as the angular or spatial decorrelation, multipath fading, or ambient noise may affect an interferometric measurement. The decorrelation phenomenon, depicted in Fig. 2, occurs when two close receivers do not see exactly the same cell resolution (spatial decorrelation *aka* sliding footprint[1]), or do not see it exactly under the same angle (angular decorrelation). Multipath fading is caused by interfering signals damaging the wavefront of the main signal. Finally, the ambient noise features several contributions such as the surface agitation, living organisms, ship traffic noise, and intrinsic noises of sonar systems (either acoustical or electrical). The more penalizing phenomena are decorrelation and ambient noise, respectively at the center and at the ends of the swath.

Thus, a classical additive model of a signal s_k received (in baseband) by the k-th sensor, composed of the contributions of p scatterers inside a resolution cell of size D_x, plus an additive noise n_k, can be written as[12,13]

$$s_k = \int_{D_x} \alpha_k(x) \exp\{j\,\phi_k(x)\}\,dx + n_k \tag{1}$$

where the phase $\phi_k(x)$ depends on the position x of the scatterers inside the resolution cell. Thus, for a large number p of scatterers, the sum of independent, identically distributed scatterers satisfies the central limit

theorem, and the resulting summation is complex Gaussian distributed. Moreover, n_k is assumed to be a white Gaussian noise inside the signal bandwidth.

Since the two interferometer receivers do not see the resolution cell under the same angle, the phases $\phi_k(x)$ are different for each receiver. Furthermore, the two receivers do not ensonify exactly the same resolution cell at the same time due to spatial decorrelation,[16] so the phase difference has to be measured over a common region (namely over $D_x - \Delta_x$ as depicted in Fig. 2). Therefore, the integration term in (1) can be split into two terms, each one corresponding to the correlated and uncorrelated part between the two receivers. Thus, the signal model (1) can be decomposed as

$$s_k = \xi_{corr} + \xi_{\overline{corr}} + n_k \tag{2}$$

where the term $\xi_{\overline{corr}}$ incorporates the whole multiplicative degradation due to both angular and spatial decorrelations as well as the path attenuation. Then, this uncorrelated part $\xi_{\overline{corr}}$ (without any useful information) and the electrical noise n_k can be merged into a unique term gathering the signal degradation. Thus, since n_k is assumed to be a white Gaussian noise and a large number of scatterers contribute to the signal backscattering, the global noise term, i.e. $\xi_{\overline{corr}} + n_k$, is assumed to be white Gaussian distributed.

Conversely, the modulus of the correlated part ξ_{corr} can be regarded as either a random or a constant variable. Finally, two signal models arise:

1) *Random-Modulus Partially-Correlated* (RMPC) signal:

$$s_1 = v + n_1 \tag{3a}$$
$$s_2 = v + n_2 \tag{3b}$$

where

$$v \sim \mathcal{N}(0, \sigma_v^2) \tag{4a}$$
$$n_i \sim \mathcal{N}(0, \sigma_n^2) \tag{4b}$$
$$s_{\mathrm{RMPC}_i} \sim \mathcal{N}(0, \sigma_i^2) \tag{4c}$$

with $\mathcal{N}(m, \sigma^2)$ denoting a Gaussian process of mean value m and variance σ^2. Linking (3) to the signal model (2), v stands for the correlated part ξ_{corr}, common to signals s_1 and s_2, whereas n_1 and n_2 are two uncorrelated, complex random processes including the contribution of the uncorrelated part $\xi_{\overline{corr}}$ and the additive noise, being different for each signal.

2) *Constant-Modulus Partially-Correlated* (CMPC) signal

$$s_1 = u + n_1 \tag{5a}$$
$$s_2 = u + n_2 \tag{5b}$$

where

$$u \sim \zeta \cdot e^{j\mathcal{U}(-\pi,+\pi)} \tag{6a}$$
$$n_i \sim \mathcal{N}(0, \sigma_n^2) \tag{6b}$$
$$s_{\mathrm{CMPC}_i} \sim \mathcal{N}(\zeta, \sigma_i^2) \tag{6c}$$

In this case, u represents the measured, useful signal whose amplitude ζ is constant, and phase is uniformly distributed within the interval $]-\pi, +\pi]$. We assume a uniform phase distribution so that the signal s_{CMPC_i} is zero-mean distributed.

In conclusion, the signal received by two sensors can be generally decomposed into a useful part behaving as either a random or a constant variable, and a noisy, random part. This theoretical modeling is now confronted to the existing interferometric statistical models and to real data collected in different underwater applications in order to verify its actual existence.

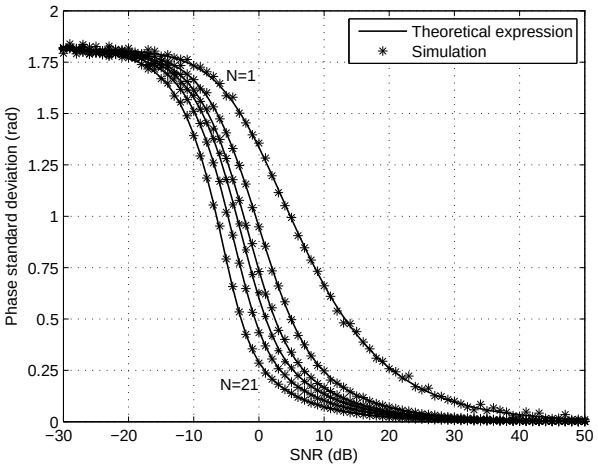

Figure 3. Prediction of the interferometric standard deviation obtained from the RMPC-signal model (3) ('*' line) compared to the theoretical interferometric variance (solid line) for $N = \{1, 3, 5, 7, 11, 21\}$.

2.3 Phenomenological analysis

The interferometric statistics derived for both electromagnetic and acoustic emitted waves have been widely studied, existing a wide literature such as Ref. 11, 13, 17, 18. Thus, signals received by the two interferometric sensors are modeled based upon a zero-mean, circular, complex Gaussian hypothesis:[11]

$$\text{Sensor 1}: \qquad s_1 = x_1 + j\, y_1 = r_1 \exp(j\, \varphi_1) \tag{7a}$$

$$\text{Sensor 2}: \qquad s_2 = x_2 + j\, y_2 = r_2 \exp(j\, \varphi_2) \tag{7b}$$

where s_k is the complex envelope issued from the analytical signal, x_k and y_k are zero-mean Gaussian distributed; amplitude r_k follows a Rayleigh distribution of parameter σ_r^2, and phase φ_k is a uniform random variable distributed on the interval $]-\pi, +\pi]$. The interferometric phase-difference estimator $\Delta\varphi$,

$$\Delta\varphi = arg\{s_1 s_2^*\} \tag{8}$$

applied to backscattered signals is unbiased, consistent and asymptotically efficient[11] as the number of independent realizations increases. The resulting interferometric-phase PDF takes the following form:[18]

$$f(\Delta\varphi) = \frac{\Gamma(N+1/2)}{\Gamma(N)} \frac{(1-|\mu|^2)^N}{2\sqrt{\pi}} \frac{\beta}{(1-\beta^2)^{2N+1/2}} + \frac{(1-|\mu|^2)^N}{2\pi}\ {}_2F_1(N, 1; 1/2, \beta^2) \tag{9}$$

where N is the number of looks, ${}_2F_1(N, 1; 1/2, \beta^2)$ is a Gauss hypergeometric function,[19] and

$$\beta = |\mu|\ \cos(\Delta\varphi - \phi) \tag{10}$$

with $|\mu|$ and ϕ being the modulus and phase of the correlation coefficient γ, computed in the single-look case as

$$\gamma = \frac{\mathbb{E}\{s_1 s_2^*\}}{\sqrt{\mathbb{E}\{s_1 s_1^*\}\mathbb{E}\{s_2 s_2^*\}}} = |\mu| \exp\{j\phi\} \tag{11}$$

It is interesting to remind the relationship[10] between the coherence $|\mu|$ and the SNR:

$$\text{SNR} = \frac{|\mu|}{1-|\mu|} \tag{12}$$

This widely-used theoretical interferometric model was compared to the RMPC- and CMPC-signal models stated in (3) and (5), respectively. Three different zero-mean Gaussian signals required in (3) were generated,

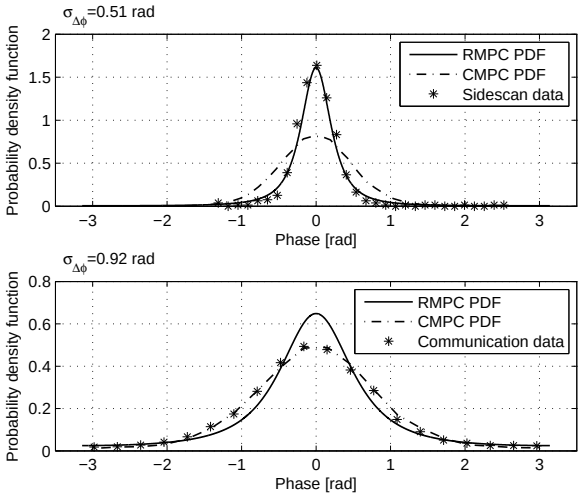

Figure 4. Experimental data phase distributions ('*' lines) checked against theoretical models (solid and dashed-dotted lines). Upper plot: evidence of RMPC behavior on interferometric sidescan sonar data sets. Lower plot: verification of the existence of CMPC signals in underwater acoustic communication applications.

their variances being tuned by the desired SNR level, in order to reproduce circular, complex, Gaussian random variables in accordance to the interferometric PDF. The standard deviation of the phase-difference estimator was computed and displayed in Fig. 3. Note the good agreement between the theoretical standard deviation (solid line) obtained through the numerical evaluation of the interferometric variance and the RMPC-signal simulation (3) ('*' line) based on a Monte Carlo method for N looks from 1 to 21. This agreement could already be expected due to the nature of the backscattered signals, namely the contribution of arbitrary number of scatterers inside the resolution cell.

The next step was to test the statistics of the two proposed types of signals to real interferometric data sets. To this end, a 455-kHz interferometric sidescan sonar was used to collect data from a 19.4-m deep flat, homogenous seafloor. The result[8] was that 84% out of 1800 range samples times 400 consecutive pings verified the RMPC-signal PDF checked on a χ^2-test. An example of PDF agreement is displayed in the upper plot of Fig. 4: the solid line corresponds to the RMPC-signal PDF, the dashed-dotted line displays the CMPC-signal PDF obtained from a Monte-Carlo simulation of signal model (5), and the '*' line depicts the PDF of 400 independent realizations of interferometric sidescan sonar data.[8] The three PDFs correspond to the same variance level, fixed by the experimental data.

In other scenarios such as underwater mobile positioning[14] or data transmission, the received signal is more stable due to the very low number of scatterer contributions, likely behaving as a CMPC signal. To verify this hypothesis, data sets were collected from a continuous-flow data transmission in an acoustic communication application between one emitter and four vertically-aligned receivers, five wavelength apart. The analysis of different blocks of the recorded signal suggests that when the reception is barely perturbed by multipath interferences, leading to a (relatively) easy equalization of the channel, the resulting interferometric signal matches the phase PDF of CMPC interferometric signals (see example in the lower plot of Fig. 4). Conversely, in a channel with an important multipath propagation, the interferometric signal behaves more like the RMPC signal model.

It is important to note that these data sets were collected for a horizontal emitter-receiver communication. In other applications such as underwater positioning, the communication is usually nearly vertical, limiting the multipath propagation from the seafloor and surface. The result is then a more stable received signal, essentially CMPC-type. Note that interferometry is not performed for itself in underwater acoustic communications; however since phase processing is currently used, the above results about phase fluctuations due to noise may be of interest for this domain.

In conclusion, both RMPC and CMPC signals are to be met in underwater interferometric applications, hence the importance of their signal-origin analysis. RMPC signals are mainly met in backscatter applications due

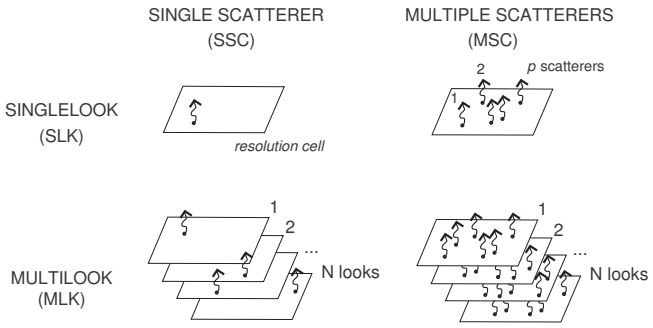

Figure 5. Nature of a single- and multiple-scatterer reflection scene under the single-look and multilook cases.

to the multiple-scatterer nature of the received signal. Conversely, the unique ray-path in applications such as underwater acoustic communications or positioning leads to a CMPC-signal behavior. These conclusions are drawn from the experimental results, but not from the addition-noise model (1). Indeed, the additive model does not take into account the number of scatterers and its distribution inside the resolution cell. It just assumed that a large number of scatterers contribute to the formation of the received signal. Conversely, in the next section, we propose a more physical noise model in order to investigate the existence of CMPC signals.

3. PHYSICAL SIMULATION MODEL

As pointed out in Section 2, the more penalizing phenomena in terms of signal degradation are the angular and spatial decorrelations, and the ambient noise. These three phenomena are merged into the following multiplicative model:

$$s_k = r_k \, e^{j\varphi_k(x)} \cdot e^{j\delta\varphi(x)} \tag{13}$$

where x allows us to model a mobile target inside a resolution cell. Thus, $\varphi_k(x)$ is the phase related to the position x of the scatterers inside the resolution cell, and $\delta\varphi(x)$ represents a possible decorrelation sketched in Fig. 1.

The statistics of this model depends on how the three variables in (13), namely r, φ_k and $\delta\varphi$, are considered. Four cases, shown in Fig. 5, are possible: there is either a single scatterer or multiple scatterers inside the resolution cell in single- or multiple looks. When a large number of scatterers reach the two sensors (independently of the number of looks), the resulting statistical distribution of s_k tends to a Gaussian process as the central limit theorem states. Therefore, the multiplicative-noise model (13) in a multiple-scatterer reflection case is in statistical agreement with the circular, complex, Gaussian model (7), and the resulting signal leads to the same performance as the RMPC-signal model (3). This means that if the CMPC-signal model (5) exists, it can only be in a single-scatterer reflection scene. Let us, then, analyze this case in a multilook scene. Thus, the single-scatterer, multilook simulation model is given by

$$s_1^i = r^i \, e^{j\varphi_1^i} \tag{14}$$

$$s_2^i = r^i \, e^{j(\varphi_2^i + \delta\varphi^i)} \tag{15}$$

$$\Longrightarrow z = \frac{1}{N}\sum_{i=1}^{N} s_1^i s_2^{i*} = \frac{1}{N}\sum_{i=1}^{N} |r^i|^2 \, e^{j\psi^i} \tag{16}$$

where x_k^i represents parameter x of sensor k at look i, and

$$\psi^i = \Delta\varphi^i - \delta\varphi^i \tag{17}$$

Compared to the additive noise model (1), the phase ψ integrates the decorrelation degradation due to the different position of the scatterer at different looks, and also the ambient noise.

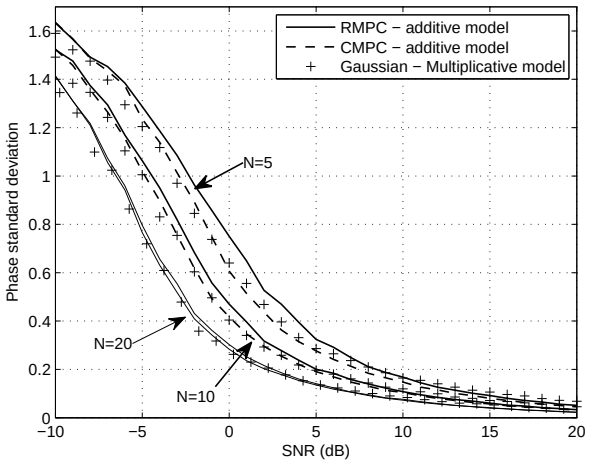

Figure 6. Phase standard deviation of signal (16) supposing its phase been Gaussian ('∘') or phase-difference ('+') distributed. Moreover, the numerical phase standard deviation of a CMPC signal (solid line) for $N = \{5, 10, 20\}$, and of a RMPC signal (dashed line) for $N = 1$ of the additive-noise model of Section 2.

An important issue comes up when the model (16) is aimed to be simulated: the statistical behavior of z is unknown. Nonetheless, since we analyze the single-scatterer case inside the resolution cell, r can be assumed constant and the same for any look i. As far as the phase ψ is concerned, a unimodal distribution such as a zero-mean Gaussian distribution makes it position to model the dispersion of the scatterer location inside the resolution cell through the increase or decrease of its variance. Indeed, a narrow sharp distribution leads to a scatterer position close to the interferometer axis, yielding a low variance, whereas a flat-shaped distribution spreads out the scatterer location. Therefore, the interferometric phase $\Delta\varphi$ issued from a single scatterer in the multilook case is numerically generated as:

$$\Delta\varphi = arg\left\{\sum_{i=1}^{N} e^{j\psi_i}\right\} \tag{18}$$

where ψ is zero-mean Gaussian distributed.

$$f_\Psi(\psi) = \frac{1}{\sqrt{2\pi}\sigma_\psi}\exp\left\{-\frac{\psi^2}{2\sigma_\psi^2}\right\} \tag{19}$$

A new issue comes up with the Gaussian assumption: no prior relation exists between the Gaussian dispersion σ_ψ^2 and the resulting phase-quality loss in terms of SNR. The link is found by roughly estimating the correlation coefficient in the multilook case as:

$$\hat{\mu}_{\text{MLK}} = \left|\mathbb{E}\left\{\frac{1}{N}\sum_{i=1}^{N} e^{j\psi_i}\right\}\right| \tag{20}$$

where MLK stands for "multilook". In order to link this estimation $\hat{\mu}_{\text{MLK}}$ with the single-look correlation coefficient given in (11) which is bijectively related to the SNR from (12), the true multilook μ_{MLK} is determined from the analytical statistics given in (7). Finally, from a given Gaussian dispersion σ_ψ^2, its connection with the resulting SNR is obtained as follows:

$$\sigma_\psi^2 \leftrightarrow \hat{\mu}_{\text{MLK}} \leftrightarrow \mu_{\text{MLK}} \leftrightarrow \mu_{\text{SLK}} \Leftrightarrow \text{SNR} \tag{21}$$

where SLK stands for "single-look".

In order to verify the right modeling of the interferometric phase (18) and the Gaussian assumption, Fig. 6 displays the RMPC- and CMPC-signal standard deviation of the additive model (in solid and dashed-dotted

lines, respectively) confronted to the standard deviation obtained with multiplicative model (in '*' lines) for $N = \{5, 10, 20\}$. This figure shows that the multiplicative noise model presents a similar standard deviation as the CMPC-signal model, but we need twice the number of looks to get this similarity:

$$var_{\text{MLP\&SSC}}\{\Delta\varphi_{\text{MLK}}\}\big|_{2N} \simeq var_{\text{AD\&CMPC}}\{\Delta\varphi_{\text{MLK}}\}\big|_{N} \tag{22}$$

where MLP and AD stand for the "multiplicative"-noise and "additive"-noise models, and SSC denotes "single scatterer". Therefore, this modeling presents promising results, proving that a widely-used Gaussian distribution can be used to generate constant-modulus signals, their existence coming up in scenarios such as Ultra-Short Baseline applications[20] where the received signal is very stable, behaving as a CMPC signal even in the single-look case as discussed in Section 2.3.

4. CONCLUSION

The understanding of the signal nature is fundamental to evaluate its statistical behavior in detection. The presence of an arbitrary number of scatterers determines the resulting fluctuation in detection. In scenarios including backscattering/reflection processes over a resolution cell, the resulting signal fluctuates according to a known distribution. These random behaviors were checked and verified in this paper through collected sidescan data.

Conversely, a direct path between transmitter and receiver reduces possible multipath effect, yielding more stable signals. This paper showed that this behavior matches quite well the proposed constant-modulus partially-correlated signal model. Furthermore, this kind of signal can also come up in applications with a single scatterer randomly moving inside a resolution cell. For this configuration, the multiplicative model presents promising results: a single Gaussian-distributed parameter achieves to integrate the phase degradation due to the random scatterer position inside the resolution cell and the additive ambient noise.

REFERENCES

[1] Lurton, X., "Swath bathymetry using phase difference: theoretical analysis of acoustical measurement precision," *IEEE J. Oceanic Eng.* **25**, 351–363 (July 2000).

[2] Massonnet, D. and Rabaute, T., "Radar interferometry: Limits and potential," *IEEE Trans. Geosci. Remote Sensing* **31**, 455–464 (Mar. 1993).

[3] Llort-Pujol, G., Sintes, C., and Lurton, X., "A new approach for fast and high-resolution interferometric bathymetry," in [*Oceans 2006 - Asia*], 1–7 (May 2006).

[4] Denbigh, P. N., "Swath bathymetry: Principles of operation and an analysis of errors," *IEEE J. Oceanic Eng.* **14**, 289–298 (Oct. 1989).

[5] Matsumoto, H., "Characteristics of SeaMARC II phase data," *IEEE J. Oceanic Eng.* **15**, 350–360 (Oct. 1990).

[6] Tribolet, J. M., "A new phase unwrapping algorithm," *IEEE Trans. Acoust., Speech, Signal Processing* **25**, 170–177 (Apr. 1977).

[7] Goldstein, R. M., Zebker, H. A., and Werner, C. L., "Satellite radar interferometry : Two-dimensional phase unwrapping," *Radio Science* **23**, 713–720 (Aug. 1998).

[8] Sintes, C. and Solaiman, B., "Strategies for unwrapping multisensors interferometric side scan sonar phase," in [*Oceans 2000 MTS/IEEE Conference Proceedings*], 2059–2065 (Sept. 2000).

[9] Llort-Pujol, G., Sintes, C., and Gueriot, D., "Analysis of vernier interferometers for sonar bathymetry," in [*Oceans 2008 MTS/IEEE Conference Proceedings*], (Sept. 2008).

[10] Jin, G. and Tang, D., "Uncertainties of differential phase estimation a associated with interferometric sonars," *IEEE J. Oceanic Eng.* **21**, 53 – 63 (Jan. 1996).

[11] Tough, R. J. A., Blacknell, D., and Quegan, S., "A statistical description of polarimetric and interferometric synthetic aperture radar data," *Proc. Royal Society* **449**, 567–589 (1995).

[12] Levanon, N., [*Radar principles*], Wiley-Interscience, New York (1998).

[13] Oliver, C. and Quegan, S., [*Understanding synthetic aperture radar images*], Artech House, Boston (1998).

[14] Watson, M., Berkowitz, J., and Wapner, M., "Ultra-short baseline acoustic tracking system," *Oceans* **15**, 214 – 218 (Aug. 1986).

[15] Stojanovic, M., "Recent advances in high-speed underwater acoustic communications," *IEEE J. Oceanic Eng.* **21**, 125 – 136 (Apr. 1996).

[16] Sintes, C., *Déconvolution bathymétrique d'images sonar latéral par des méthodes intérferométriques et de traitement de l'image*, PhD thesis, Université de Rennes I, France (Nov. 2002).

[17] Goodman, N. R., "Statistical analysis based on a certain multivariate complex gaussian distribution (an introduction)," *The Annals of Mathematical Statistics* **34**, 152–177 (Mar. 1963).

[18] Lee, J. S., Miller, A. R., and Hoppel, K., "Statistics of phase difference and product magnitude of multilook processed gaussian signals," *Waves in Random Media* **4**, 307–319 (July 1994).

[19] Abramowitz, M. and Stegun, J. A., [*Handbook of Mathematical Functions*], Dover Publications Inc. (1972).

[20] Beaujean, P. P. J., Mohamed, A. I., and Warin, R., "Maximum likelihood estimates of a spread-spectrum source position using a tetrahedral ultra-short baseline array," in [*Oceans 2005 MTS/IEEE Conference Proceedings*], **1**, 142 – 146 (June 2005).